NASA
National Aeronautics and Space Administration

PROCEEDINGS OF

1ST INTERNATIONAL HYPERSONIC WAVERIDER SYMPOSIUM

OCTOBER 17-19, 1990

UNIVERSITY OF MARYLAND
COLLEGE PARK, MARYLAND, U.S.A.

Sponsored by:

The National Aeronautics and Space Administration

and

The Department of Aerospace Engineering
University of Maryland

Efficient Waveriders from Known Axisymmetric Flow Fields.

J.Pike
Cranfield Institute of Technology

Summary

A design method for complete waverider configurations for which the flow field is known forward of the trailing edge at a prescribed Mach number and incidence was described by Jones, Moore, Pike and Roe in 1968. The lower surface shapes used to demonstrate the method were derived from cone cylinder flows which contained only limited potential for adapting the surface shape. As the lower surface provides most of the lift and drag, it is desirable for it to have a good lift to drag ratio, as well as being able to accomodate other geometric constraints.

The range of compression surfaces has been increased by investigating surfaces from axisymmetric flows with curved shock waves. This permits the anhedral, semi-span to length ratio and fore and aft pressure distribution to be varied in a systematic way to improve the lift to drag ratio. Optimisation of the shape with an estimate for skin friction gives guidance as to desirable anhedral and semi-span to length ratios.

The amount of axisymmetric influence on the cross-flow near the wing tips is investigated to improve the lift to drag ratios as well as the centre line pressure distribution. An improvement in the equivalent lift to drag ratio of the lower surface of nearly 20% is achieved, giving for example a lower surface with an inviscid lift to drag ratio of 11.1 for a lift coefficient of 0.057 at Mach 4. It is also found that volume can be added to this configuration near the nose such that the lift to drag ratio is not seriously degraded.

1. Introduction.

During the 1960's the waverider* concept was developed to produce integrated configurations [1-5], such as that shown in figure 1. These shapes were produced by combining stream surfaces which support known flow fields, a method which has the advantage that at the particular design Mach number and incidence the lift and pressure drag of the configuration can be calculated exactly. Although twenty years have passed, this simple technique still has relevence today, in that it enables the effect of certain systematic shape changes to be assessed without the uncertainty associated with approximate aerodynamic theories. It should be noted that much of the work reported here was done during the 1970's when the author was employed at the Royal Aerospace Establishment, Bedford, UK.

Although the configuration shown in figure 1 was aimed at producing an efficient high supersonic Mach number cruise vehicle, the investigations are also relevent to the performance of shuttles at hypersonic speeds, when the lift to drag ratio is important. The aim here is to try and understand the type of shape which will give high lift to drag ratios and the penalty for deviating from these shapes, rather than trying to find an optimum shape for some set of constraints. From consideration of figure 1 or otherwise, it is clear that at high supersonic or hypersonic speeds most of the aerodynamic lift comes from the lower surface. Therefore, to obtain a high lift to drag ratio it is important that this lift is produced without producing excessive drag. For configurations where the lower surface shock wave is attached or nearly attached to the leading edge, the upper and lower surface flows are nearly independent and the lift to drag ratio of the lower surface may be assessed independently of the upper surface flow.

Using various aerodynamic theories a number of optimum lifting surfaces have been found for a variety of constaints [6,7]. However interesting these optimum shapes maybe, there remains a doubt about the validity

of the optimum due to the assumptions made in developing the aerodynamic theory. Also practical lifting surfaces at best resemble the optimum shape and there is a need to know the penalty from deviating from the optimum. It is useful then to assess more generally the type of shape or particular feature of the shape which gives good lift to drag ratios and the penalties incurred when these features are eroded. An obvious example is the amount of anhedral that the wing should have. It is accepted that some anhedral is desirable to "contain" the lower surface flow, but that the amount of anhedral of a caret wing supporting a plane shock wave tends to be too large for the best lift to drag ratios [8]. The variation of the lift to drag ratio with the anhedral is investigated in the present paper.

When considering a systematic variation of the shape such as that of the anhedral above, any improvement in the lift to drag ratio has to take account of the change in the lift coefficient of the surface. As a reference we use the change in the lift to drag ratio given by a two-dimensional wedge, which happens to have the same invisid performance as a caret wing supporting a plane shock wave. The lift to pressure drag ratio can be expressed as a function of the lift coefficient from oblique shock wave theory as

$$L/Dp=(2/C_L-1)[4M^2/(4M^2-4-(\gamma+1)M^2C_L)-1]^{1/2} \qquad (1)$$

This relationship is plotted in figure 2 for a Mach number (M) of 4, a ratio of specific heats (γ) of 1.4 and for lift coefficients (C_L) of up to 0.2. It may be extended to viscous flows by using a mean skin friction drag,

i.e $$L/D = C_L/(C_{Dp}+S_W C_f) \qquad (2)$$

where S_W is the wetted area over the plan area and C_f is is the mean skin friction coefficient.

2. Flow field variation.

The flow field used to design the lower surface of the configuration shown in figure 1, is the flow about a 15^o cone-cylinder as shown in figure 3. The

streamline which forms the lower surface ridge line is shown (upside down) in figure 3, with an inflexion point indicated at the start of the cone-cylinder expansion. Forward of this point the streamline is influenced by the cone only and the surface is concave. Aft of this point the streamline is influenced by the expansion from the start of the cylinder and the ridge line is convex. The pressure distribution along the ridge line is shown below the flow field. The pressure is the normal cone flow pressure distribution until the inflexion point, aft of which the cylinder expansion causes a sudden drop in the pressure. The lift over pressure drag for the lower surface which is 6.9 is plotted against the wedge performance curve of figure 2 at a lift coefficient of 0.083, where we can see from the position of the cross below the wedge curve that the efficiency of the surface from this flow field is poor. From inspection of the pressure distribution in figure 3, we see that a large area near the base of configuration is contributing little to the lift, which must be expected to result in a poor performance of the surface.

To systematically investigate the changes in the lift to drag ratio with surface shape, we select stream surfaces from the flow behind axisymmetric shock waves with more general curved profiles. The shock wave shape is described by the shock wave inclination to the free stream flow direction (θ) where

$$\theta = \theta_B + (\theta_N - \theta_B)[(1-Y)/(1-R)]^n \qquad R<Y<1 \qquad (3)$$

The angles θ_N and θ_B are the shock inclination at the nose and base respectively as shown in figure 4. The radial distance R is the distance of the nose from the axis of symmetry and Y varies from R to 1 in equation 3 to define the shock wave shape. By varying the parameters θ_N, θ_B, R and r (the shock curvature index) the shock shape can be systematically varied. The flowfield downstream of the shock was calculated using a program based on the method of characteristics written by K.C.Moore [9].

As a typical example of a flow field we set θ_N as 22^o, θ_B as 18^o, R at 0.1 and n equal to 2. This gives

the flow field shown in figure 5. The associated pressure distribution is shown below the flow field to be very different to that of figure 3. When the planform is prescribed to be a delta with a semi-span to length ratio of 0.3, the compression surface from the flow field is shown in figure 6. This has a much higher lift to drag ratio than the compression surface from figure 1 but a lower lift coefficient. When the lift to drag ratio is compared to the standard wedge curve of figure 2, we see that although much of the increase in the lift to drag ratio is due to the smaller lift coefficient, the lift to drag ratio of this surface is close to the wedge value, suggesting that it is a more efficient lift producer.

3. Efficient lifting surfaces

The plane two-dimensional wedge is used here as a reference for comparing the efficiency of compression surfaces which have different lift coefficients and friction drag. Many aerodynamic theories (including linear, Newtonian and tangent-wedge theories), predict that this shape is optimum for two-dimensional flows; that is it gives the maximum lift to drag ratio for a given lift. Using hypersonic small disturbance theory however, Cole and Aroesty [10] suggest that the (invisid) optimum is a multi-wedge. It has been shown further using the more generally applicable Busemann second order theory applied to the flow behind the wedge shock wave [11], that the optimum inviscid two-dimensional shape is a double wedge, which is slightly concave for Mach numbers greater than 3. This result can also be shown to hold for hypersonic small disturbance theory and Cole and Aroesty's multi-wedge shape should reduce to a double wedge. The improvment in the lift to pressure drag ratio that can be obtained using a double wedge can be found without approximation from oblique shock wave theory. The increase in the lift to drag ratio is found to be only one or two percent greater than the plane wedge however and we may justifiably continue to use the plane wedge for comparison purposes.

The two-dimensional optimum is perhaps surprising in that a two-dimensional isentropic compression is

known to be a more efficient means of raising the pressure than a shock wave. However to use an isentropic compression in two-dimensional flow requires a region of the surface near the nose with a smaller inclination and pressure. The optimum result thus indicates that except for some small effects, the losses from the variation of the surface slope and the pressure when using an isentropic compression are greater than the gains available from the more efficient compression. This shape disadvantage when using two-dimensional isentropic compressions need not apply to three-dimensional flows however. For example, if we consider the flow about an unyawed cone, the shock wave and the surface have straight longditudinal profiles, but in the flow between the shock wave and the cone surface the pressure is raised by an isentropic compression caused by the lateral compression of the flow as it approaches the axis. This lateral compression is common to all axisymmetric flows and provides a mechanism by which the efficiency of compression surfaces might be improved. We can isolate this effect from other complicating features by considering the lift to pressure drag ratio of very narrow wings obtained from axisymmetric flow fields.

If in equation 3, θ_N is set equal to θ_B and R is set to 0 or 1, the flow field becomes that about a cone or wedge respectively. These flow fields represent extreme cases of the flow fields from equation 3, but they can be used to demonstate the performance gain available from axisymmetric flows. The lift to pressure drag ratio of compression surfaces from a cone flow where the cone has a 10^o semi-apex angle are shown by the upper solid line in figure 7. A typical section through a compression surface is shown above this line. The values shown are for wings with small semi-span to length ratios (s/l). As the semi-span is increased the lift to pressure drag ratio decreases by a factor $(s/l)\cot\theta_B/\sin^{-1}((s/l)\cot\theta_B)$ which is shown as a function of s/l in the lower plot. The lift to drag ratio of compression surfaces which have the same lift coefficient as the cone wing but for which R is equal to one are shown by the dotted line. This line can represent a caret wing with the same s/l as the cone wing, or, more significantly, the lift to pressure drag

ratio of the reference two-dimensional wedge. We see then that for the whole of the Mach number range, narrow cone wings have a better lift to pressure drag ratio than a wedge. The lower solid line in figure 7 shows the lift to pressure drag ratio of cone wings when the plane through the leading edges is tangent to the cone surface. These wings demonstrate that the loss of efficiency for less narrow wings is also similar across the Mach number range.

Although the cone compression surfaces are interesting for illustrative purposes, the main interest lies with the more practical shapes which are produced when Θ_N is greater than Θ_B and R is between 0 and 1. An example of such a compression surface has already been shown in figure 6. These compression surfaces exhibit trends which are similar to those of the cone wings as can be seen in figure 8. The axisymmetric flow used to obtain the compression surfaces in this figure is the one already shown in figure 5. Consider, for example, the left most configurations at the top of figure 8 which have a small semi-span to length ratio. We see immediately from to uppermost curve, that for these narrow wings (near the vertical axis of the figure) the lift to pressure drag ratio is significantly above the plane two-dimensional wedge value (shown dotted). We see also from figure 8 that increasing the semi-span to length ratio results in a reduction in the lift to pressure drag ratio and the efficiency of the compression surface, as predicted by the cone wing. This effect can be explained using Roe's inviscid streamtube efficiency analysis [5], as being caused by inefficient streamtubes near the wing tips, where as the semi-span to length ratio increases, the curved shock wave gives progressively more lateral momentum to the flow.

The inclusion of friction drag has a large impact on these results. Compression surfaces with small semi-span to length ratios have large amounts of anhedral. When friction drag estimates are introduced, the large surface area to planform area ratio (Sw) reduces the lift to drag ratio of these wings (see equation 2), such that as the semi-span tends to zero the anhedral angle tends to 90^o and the lift over drag

ratio also tends to zero. Thus the most efficient wings strike a balance with increasing semi-span to length ratio, between the less efficient inviscid performance and the decreasing friction drag. This is shown in figure 8 by the three lower curves which have mean friction drag coefficients of 0.001, 0.002 and 0.004 respectively. We see that the efficiency of the compression surfaces reaches a maximum when the semi-span to length ratio is between 0.25 and 0.3 representing anhedral angles of about 20^{o} to 30^{o}. The compression surface shape for a semi-span to length ratio of 0.3 is shown in figure 6. This shape has a lift to drag ratio very close to the two-dimensional wedge value shown in figure 2, without the excessive anhedral and subsiquent loss of efficiency associated with the compression surfaces derived from two-dimensional flows.

In figure 7 results for R equal to zero and one were presented for a range of Mach numbers. In figure 8 the variation of semi-span to length ratio was investigated for a curved shock flow with R equal to 0.1. A continuous variation of the annular radius from full axisymmetric (R=0) to two-dimensional (R=1) is shown in figure 9. The longditudinal shock profile is maintained the same shape as that of figure 8, with $\theta_N=22^{0}$, $\theta_B=18^{0}$ and r=2 and the Mach number and semi-span to length ratio are fixed at 4 and 0.3 respectively. The lift to drag ratios for skin friction coefficients of 0.001 and 0.002 are compared with the with the wedge lift to drag ratios which are shown by the dotted line. We see that the best performance occurs with the annular radius (R) at about 0.2. The compression surface shown in figure 6 has an annular radius of 0.1, which can be seen from figure 9 to be close to the best lift to drag ratio. Below the performance plot is shown the anhedral of the compression surface. We see that for nearly two-dimensional compression surfaces the anhedral is large and that the efficiency of the wing is degraded by the friction drag. For full axisymmetric compression surfaces when R=0 the anhedral is small. However a small anhedral is less efficient at containing the flow and results in large lateral shock inclinations near the wing tips. This introduces a region of inefficient

flow near the wing tips which counteracts the efficient flow near the plane of symmetry of the compression surface caused by the lateral isentropic compression. This results in the loss of efficiency near the axis in figure 9.

The search for efficient lifting shapes introduces features which may not be desirable for practical configurations. One such example is the volume near the nose. Efficient lifting surfaces with attached shock waves tend to have ridge line inclinations at the nose which are the same or smaller than the average inclination of the surface. This effect can be seen for the compression surfaces of figures 1 and 6 from the ridge line shapes which are shown in figures 3 and 5. To increase the volume near the nose the ridge angle is increased locally by varying the initial shock angle in equation 3. In figure 10 the performance of compression surfaces with a semi-span to length ratio of 0.3 is shown, where the initial shock angle is increased progressively from 18^{o} to 30^{o}. This gives a variation (at M=4) of initial ridge angle from just over 5^{o} to nearly 18^{o}, as indicated at the top of the figure. We see that as the nose angle is increased the lift to drag ratio slowly falls. However the increase in the inclination at the nose also affects the lift and when the lift to drag ratio is compared with the equivalent two-dimensional wedge (shown dotted), we see that the efficiency of the wing is changed very little.

The flow field with an initial shock angle of 30^{o} is shown in figure 11 with the pressure along the body plotted below. Compared with the flow field of figure 5 that the pressure is much higher near the nose but that it rapidly reduces to a pressure close to that of figure 5. A compression surface from the flow field of figure 11 with a semi-span to length ratio of 0.3 is shown in figure 12. Away from the nose the most obvious difference in shape between the compression surfaces of figure 6 and 12 is the increase in anhedral in figure 11. This is caused by the initially large shock angle expanding the radial shock distance downstream, giving an effective positive increment to the nose radius R. As we have seen from figure 9, increasing the nose radius above 0.1 gives a slight increase in the lift to

drag ratio which will partially off-set the loss of lift to drag ratio due to the blunter nose. Even although figure 11 shows there is little loss of efficiency for an initial nose angle increase from 5^{o} to 18^{o}, it cannot be assumed that much greater nose angles or blunt noses will not cause significant performance loss. In particular for blunt noses there will be more drag without the compensating lift increment.

4. Further work

The investigation of axisymmetric flows has identified effects which influence the efficiency of the compression surfaces. Further improvements in the lift to drag ratio might be achieved by using non-delta planforms or non-axisymmetric flows. A typical modified planform shape is the ogive shape shown in figure 1. Other planform shapes include blunt or planforms with swept trailing edges. Ogive planforms tend to increase the anhedral near the wing tips, which reduces the inefficient flow region there but increases the friction drag. This can result in a small increase in the lift to drag ratio. Blunt planforms may increase this effect. It has been shown [12] for cone flow compression surfaces of given lift, that blunt planforms are optimum. Whether such planforms are optimum for given lift coefficient and other flows remains unclear. Sweeping the trailing edge in figure 1 would increase the lift to drag ratio significantly by reducing the effect of the non-lifting region near the base, however for more efficient compression surfaces such as that of figures 6 or 11 the effect would be smaller.

Of more interest is the prospect of altering the efficiency by using non-axisymmetric flows. One such flow which has been investigated is conical non-axisymmetric flow [13,14]. This introduces the prospect of controlling the shock wave shape to perhaps increase the lateral compression near the plane of symmetry while reducing the lateral shock inclination outboard. Further examples of conical waveriders are needed however to assess whether such shock shapes can improve the efficiency significantly.

5. Conclusions

A wide range of compression surfaces from axisymmetric flow fields with a prescribed shock wave shape have been computed. These surfaces have been used to assess changes in the lift to drag ratio with surface shape and to identify the aerodynamic reasons for these changes. Variation in the fore and aft profile, the lateral profile, the nose angle and the degree of two-dimensionality are investigated. It is found that good lift to drag ratios can be achieved by balancing the efficient lateral compression of the flow near the axis of symmetry with the inefficiency of high lateral shock inclination near the wing tips and the large friction drag due to excessive surface inclination to the horezontal.

The lift to drag ratios at different lift coefficients are compared by refering them to the lift to drag ratio of a plane two-dimensional wedge. When a realistic friction drag is included, it is found that the wedge gives a good estimate of the best lift to drag ratios achievable using axisymmetric flows. For these high lift to drag ratio compression surfaces it is demonstated that there still remains shape changes which can be implimented without significantly degrading the lift to drag ratio.

References

1. Jones J.G., Moore K.C., Pike J. and Roe P.L. A Method for Designing Lifting Configurations For High Supersonic Speeds Using Axisymmetric Flow Fields. Ingenieur-Archiv, 37. Band, 1. Heft, 1968, S.56-72.
2. Jones J.G. A method of designing lifting configurations for high supersonic speeds using the flow fields of non-lifting cones. A.R.C R.& M. 3539. March 1963.
3. Moore K.C., The application of known flow fields to the design of wings with lifting upper surfaces at high supersonic speeds. R.A.E. Tech. Report 65034. Feb 1965.
4. Pike J., A design method for aircraft basic shapes with fully attached shock waves using known axisymmetric flow fields. R.A.E. Tech. Report 66069. March 1966.
5. Roe P.L., A Momentum Analysis of Lifting Surfaces in Inviscid Supersonic Flow. A.R.C. R.& M. 3576. May 1967.
6. Miele, A., (Editor) Theory of Optimum Aerodynamic Shapes. Academic Press, New York 1965.
7. Nastase, A., Wing Optimisation and Fuselage Integration for Future Generation of Supersonic Aircraft. Collection of papers, 26th Israel Annual Conference on Aviation and Astronautics, Israel February 1984.
8. Pike J., The Pressure on Flat and Anhedral Delta Wings with Attached Shock Waves. The Aeronautical Quarterly, V. XXIII, Part 4, Nov 1972.
9. Moore K.C., Private Communication.
10. Cole J.D. and Aroesty J., Optimum hypersonic lifting surfaces close to flat plates. AAIA J. Vol. 3,No. 8, p. 1520, Aug 1965.
11. Pike J., Minimum Drag Surfaces of given Lift which Support Two-Dimensional Supersonic Flow Fields. A.R.C. R.& M. 3543. Sept 1966.
12. Kim B.S., Rasmussen M.L. and Jischke M.C., Optimization of Waverider Configurations Generated from Axisymmetric Conical Flows. AIAA-82-1299, AIAA 9th Atm. Flight Mech.Conf. Aug. 1982.
13. Pike J., On Conical Waveriders. R.A.E Tech. Report 70090. May 1970.

14. Rasmussen M.L., Waverider Configurations Derived from Inclined Circular and Elliptic Cones. J. of Spacecraft and Rockets, Vol. 17, No. 6, Nov.-Dec. 1980, pp. 537-545.

	C_L	$(\frac{L}{D})$ inviscid
Lower surface	0·083	6·9
Upper surface	0·020	14·8
Total	0·103	7·7

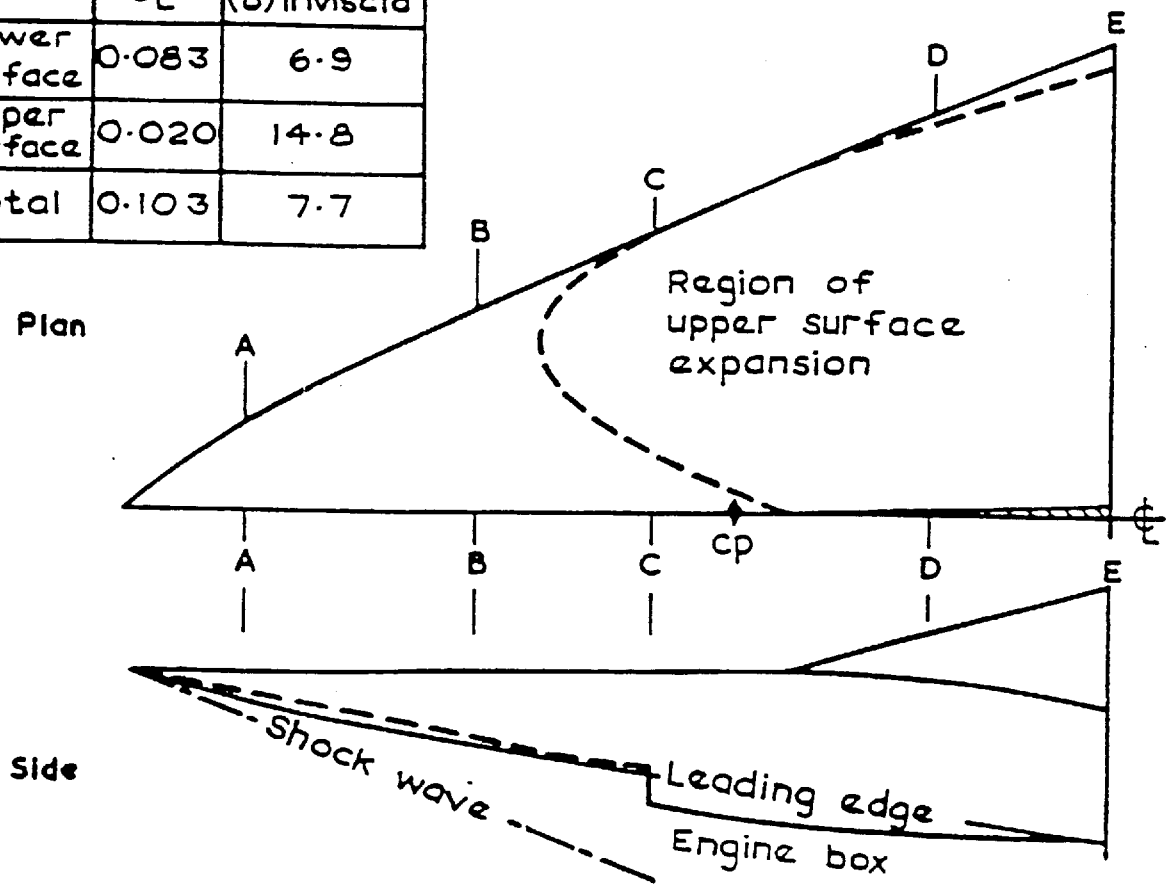

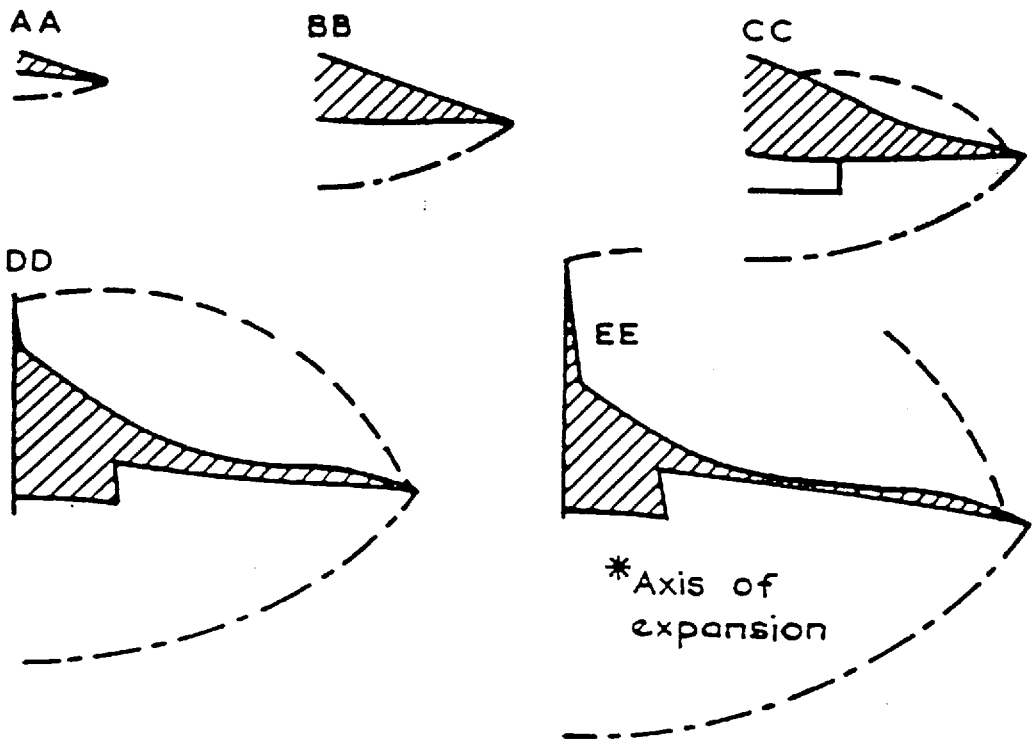

Fig. 1 An integrated aircraft configuration

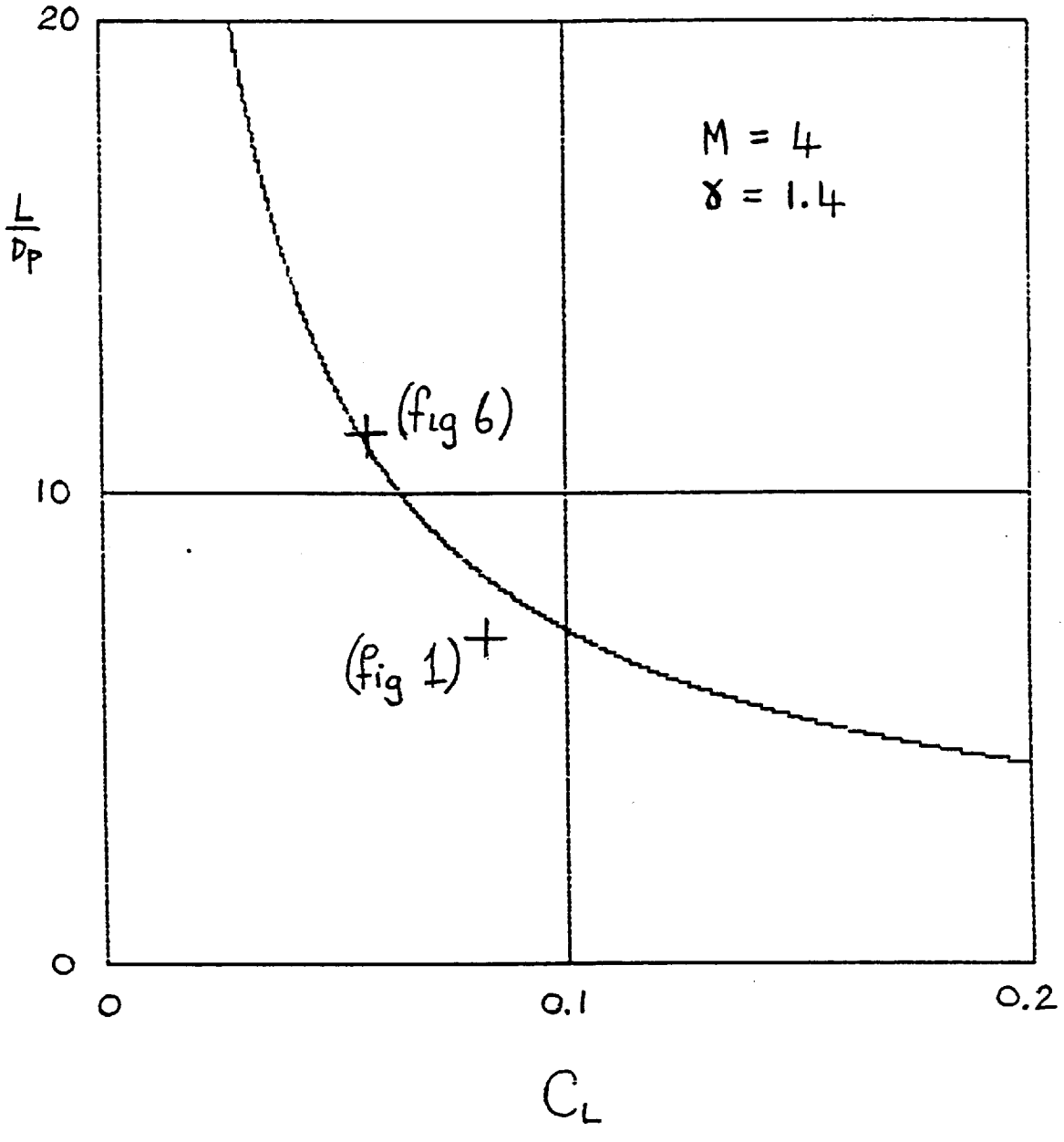

Fig. 2 Lift to drag ratio of a wedge

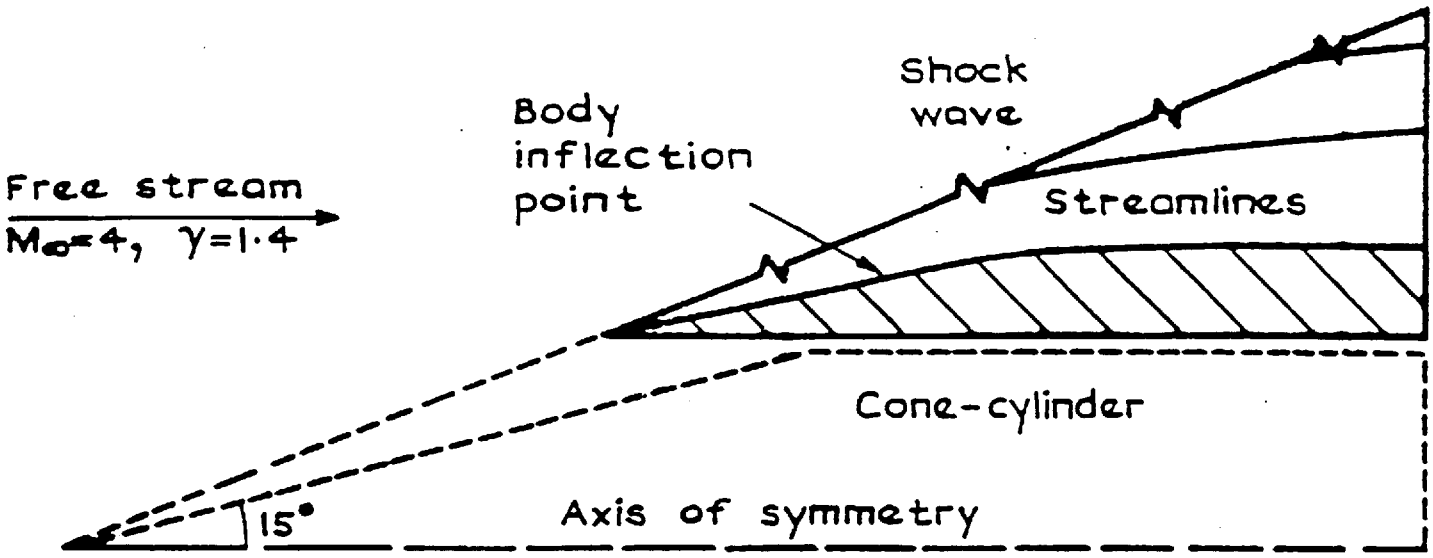

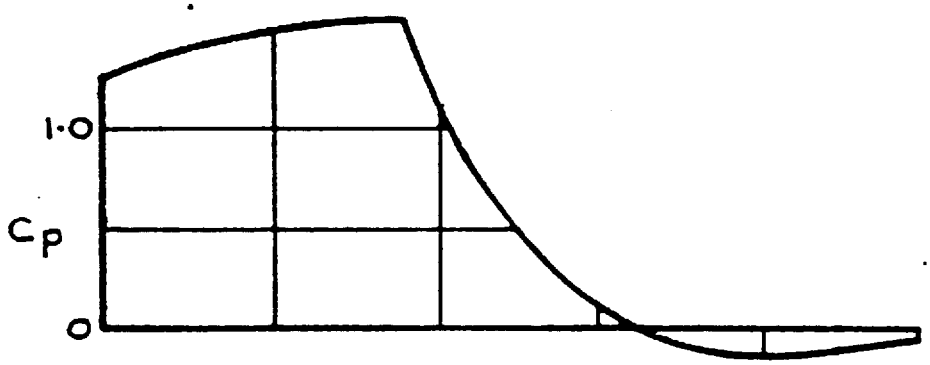

Pressure coefficient along body

Fig. 3 Cone–cylinder flow field used to design Fig. 1

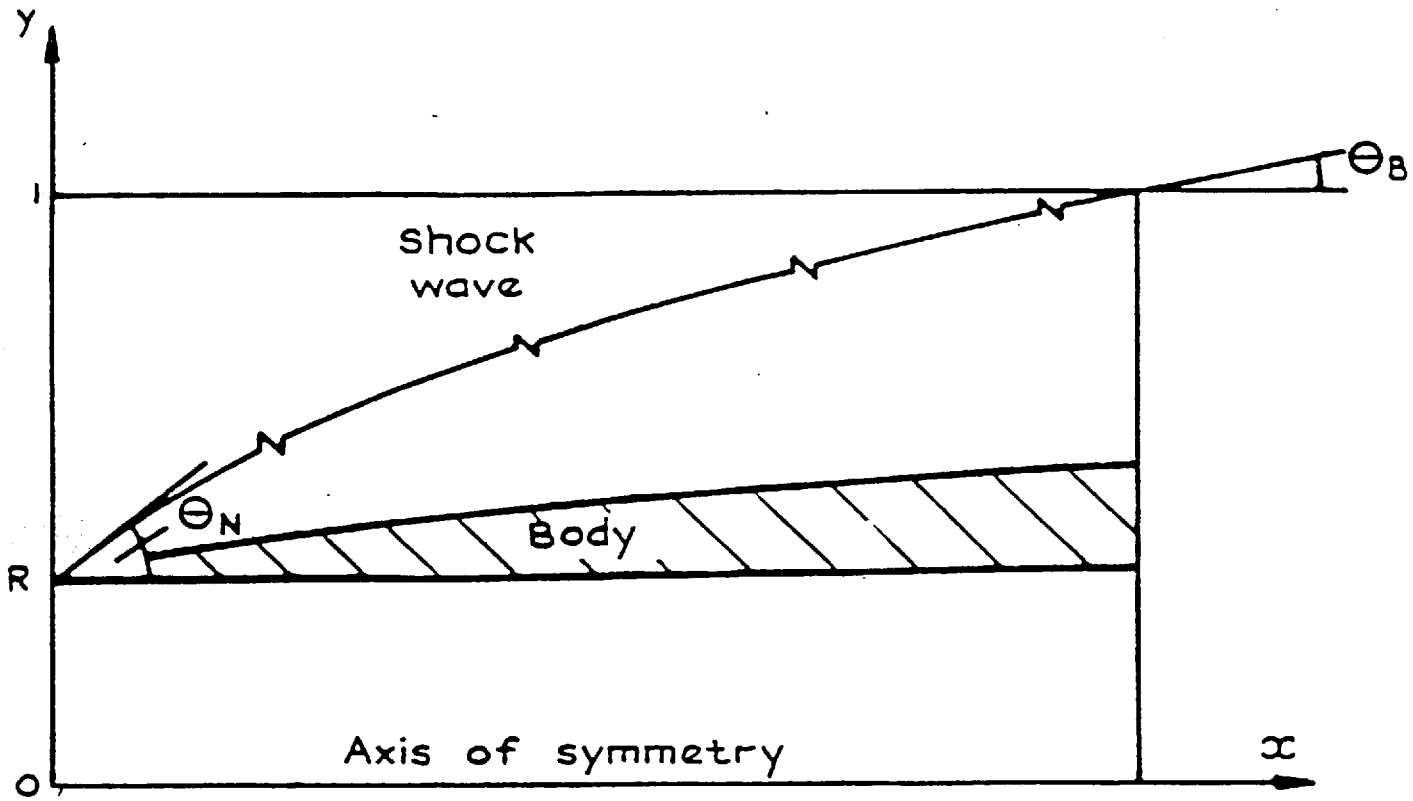

Fig. 4 Shock wave parameters Θ_N, Θ_B and R

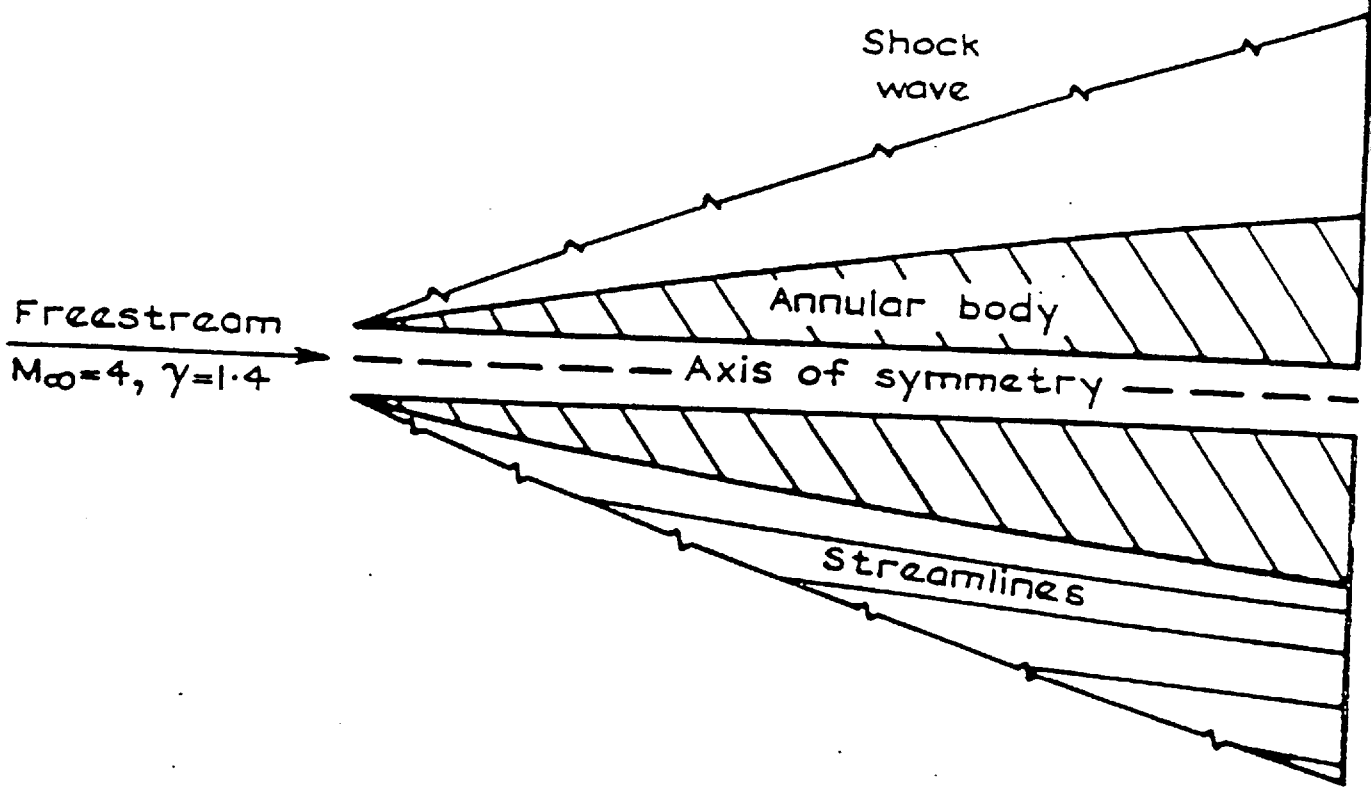

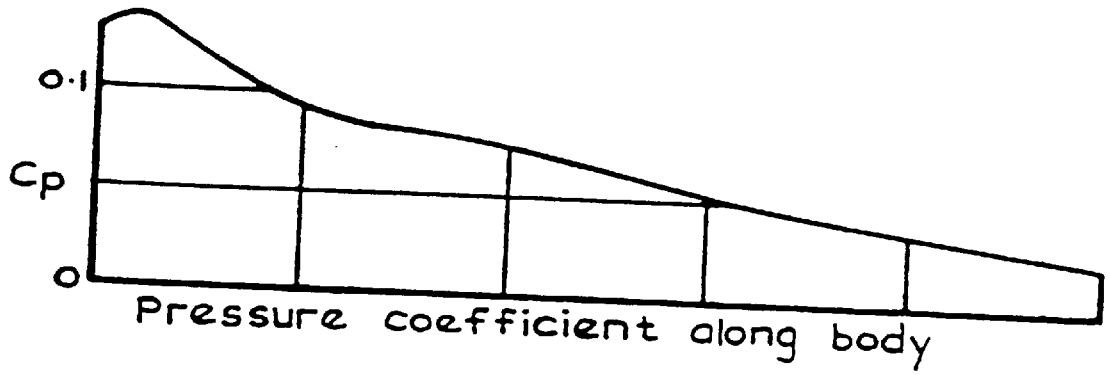

Fig. 5 A calculated axisymmetric non-homentropic flow field

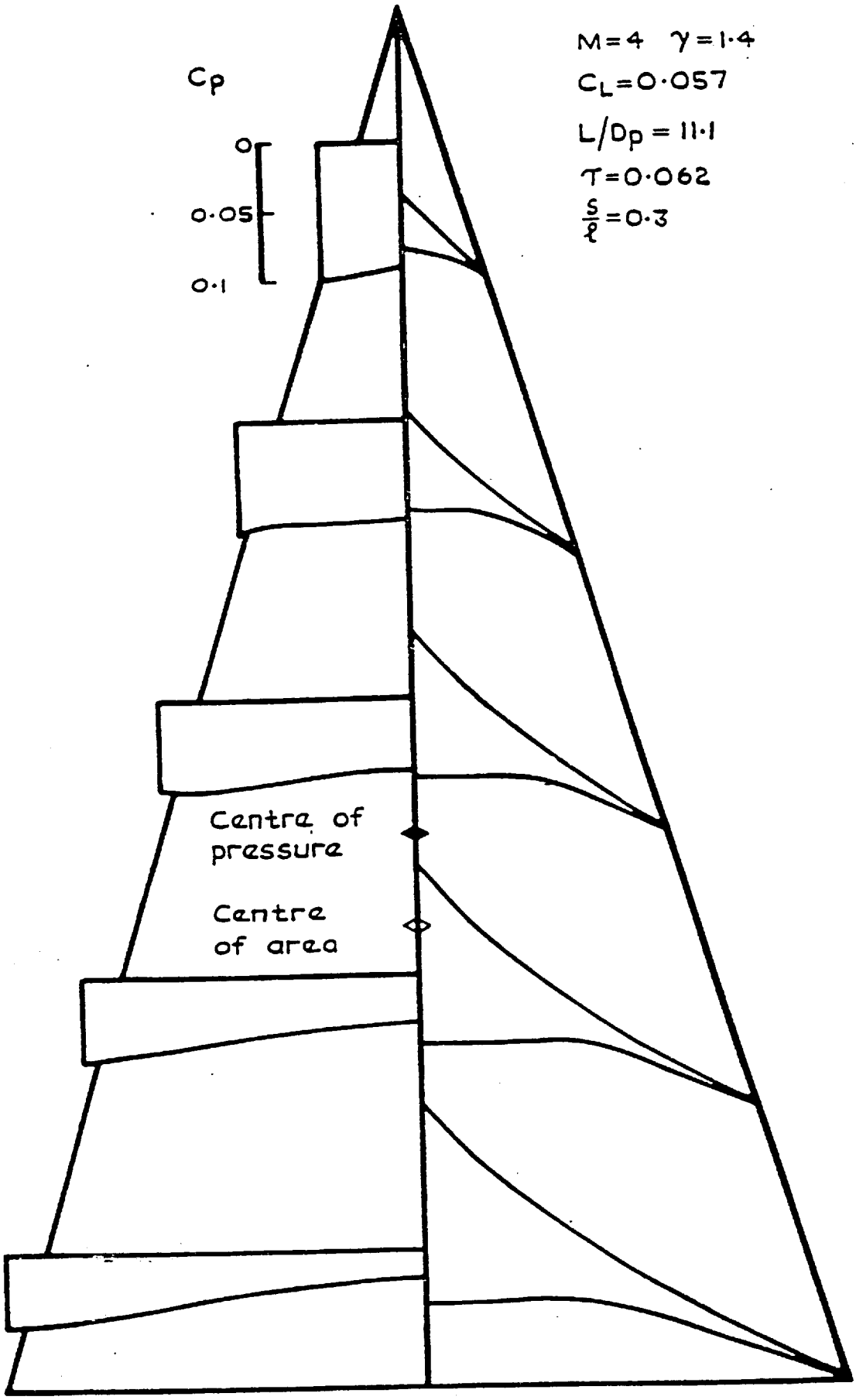

Fig. 6 Pressure distribution and sections of a configuration derived from the flow field shown in Fig. 5

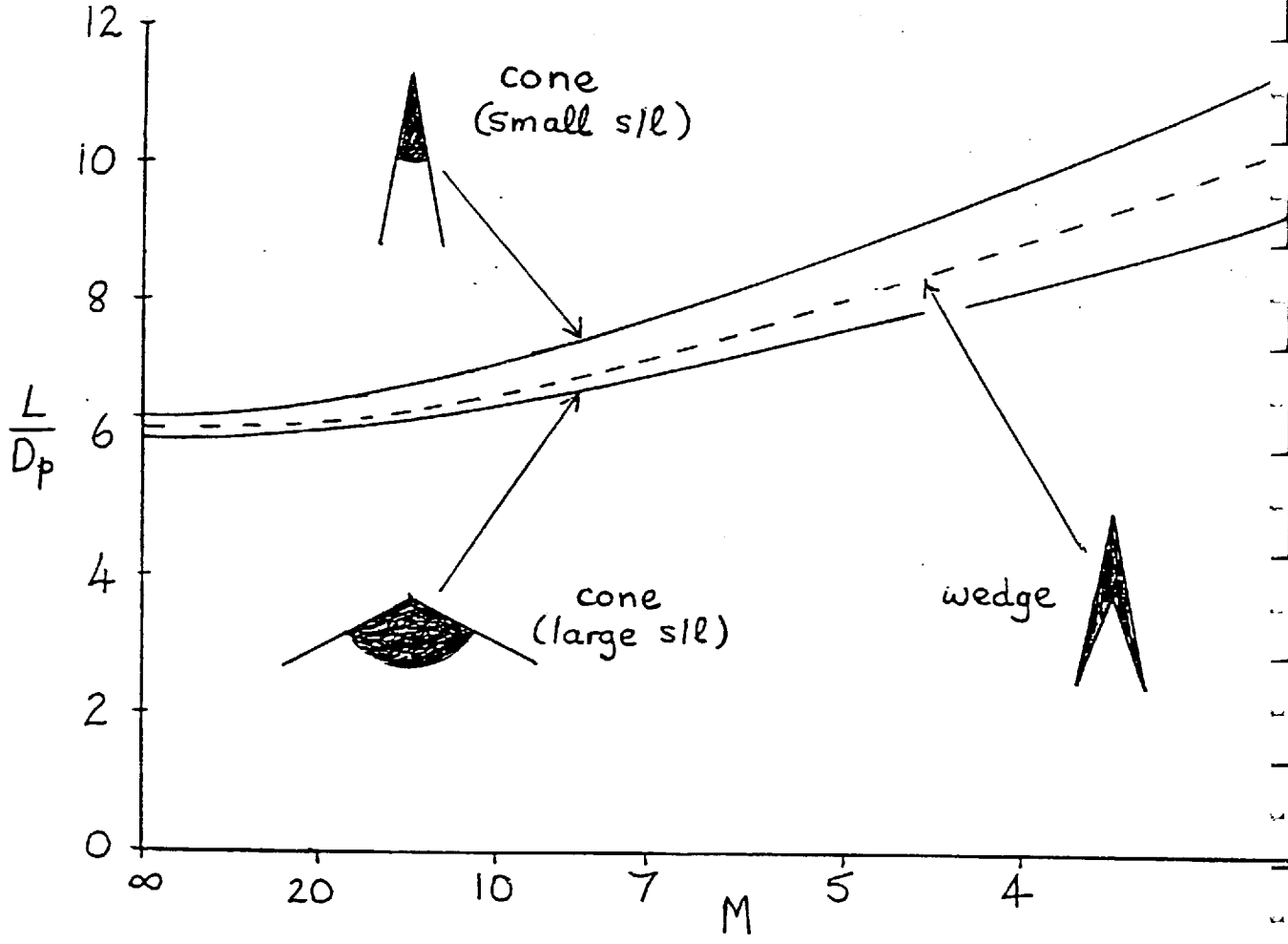

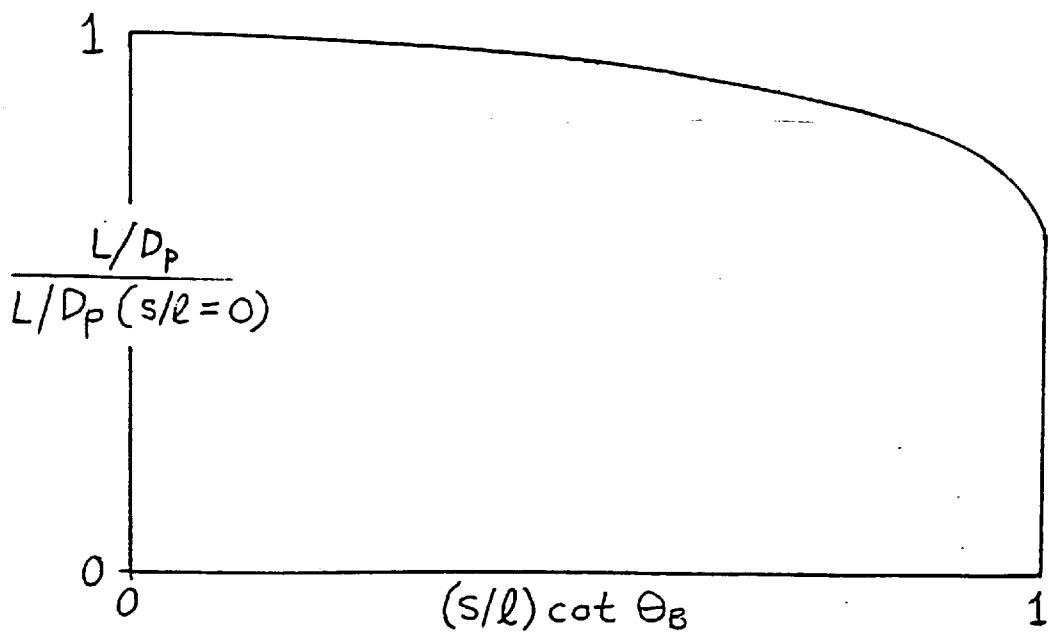

Fig 7 Lift to pressure drag ratio of 10° cone wings

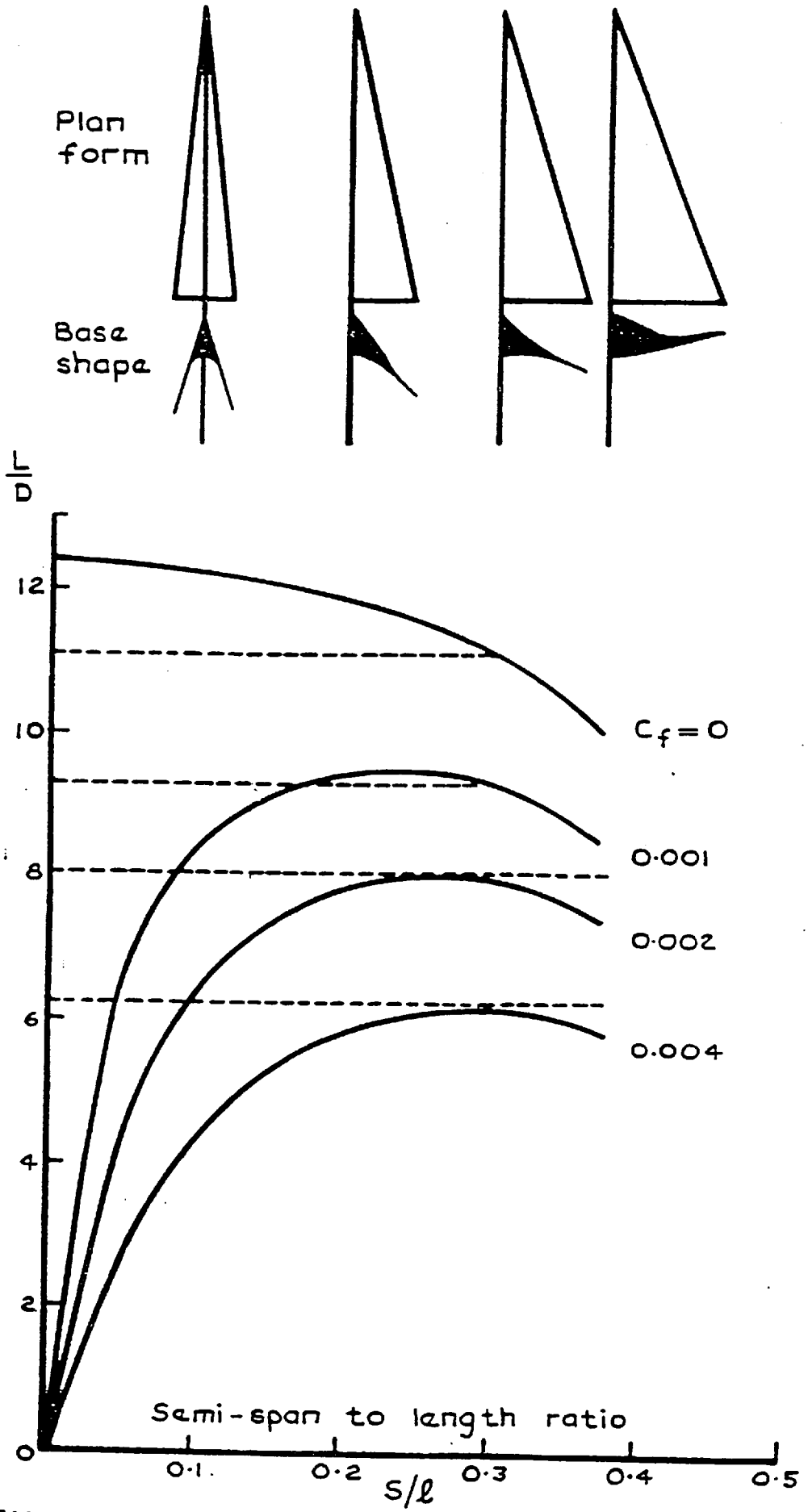

Fig. 8 Effect of semi-span to length ratio on shape and L/D

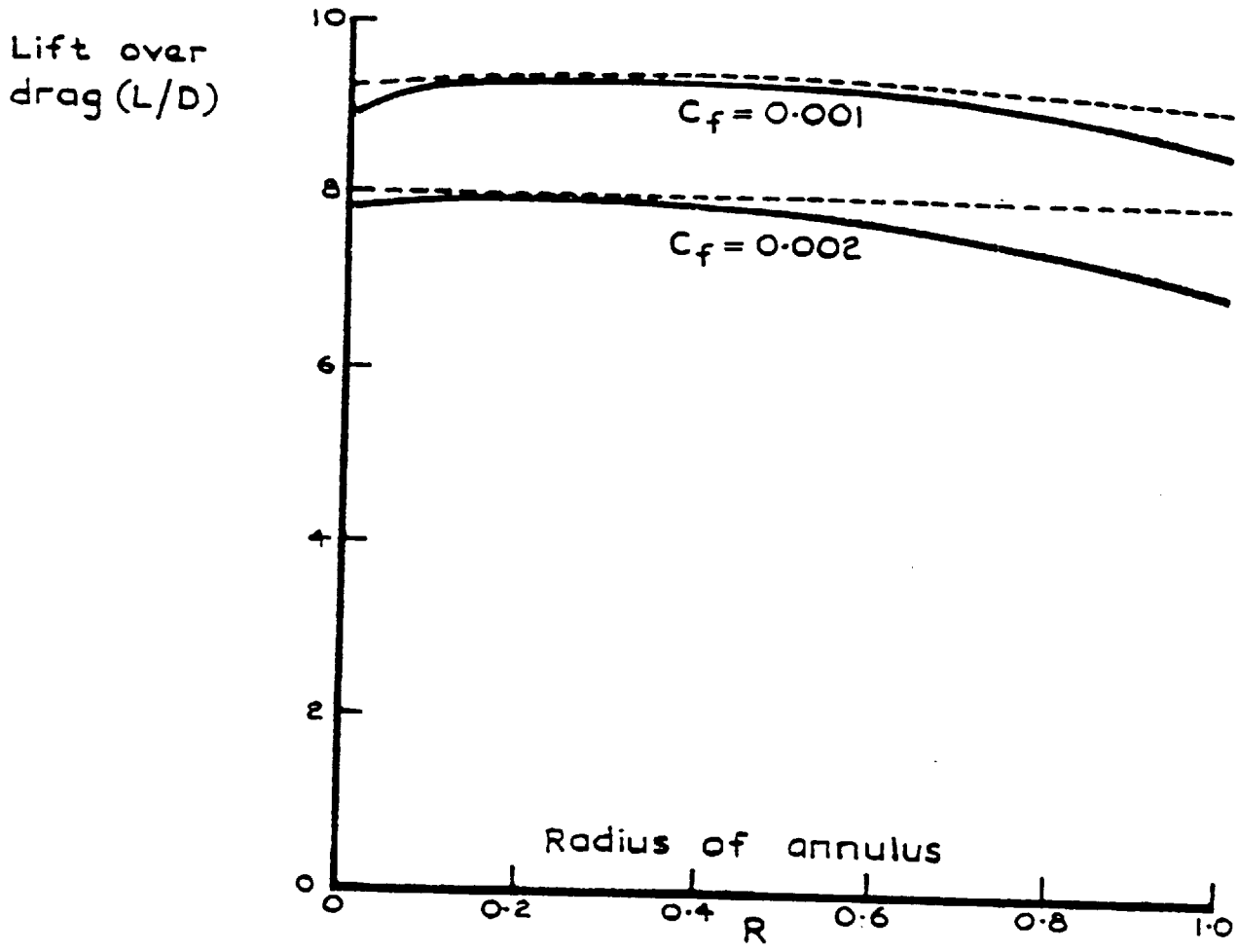

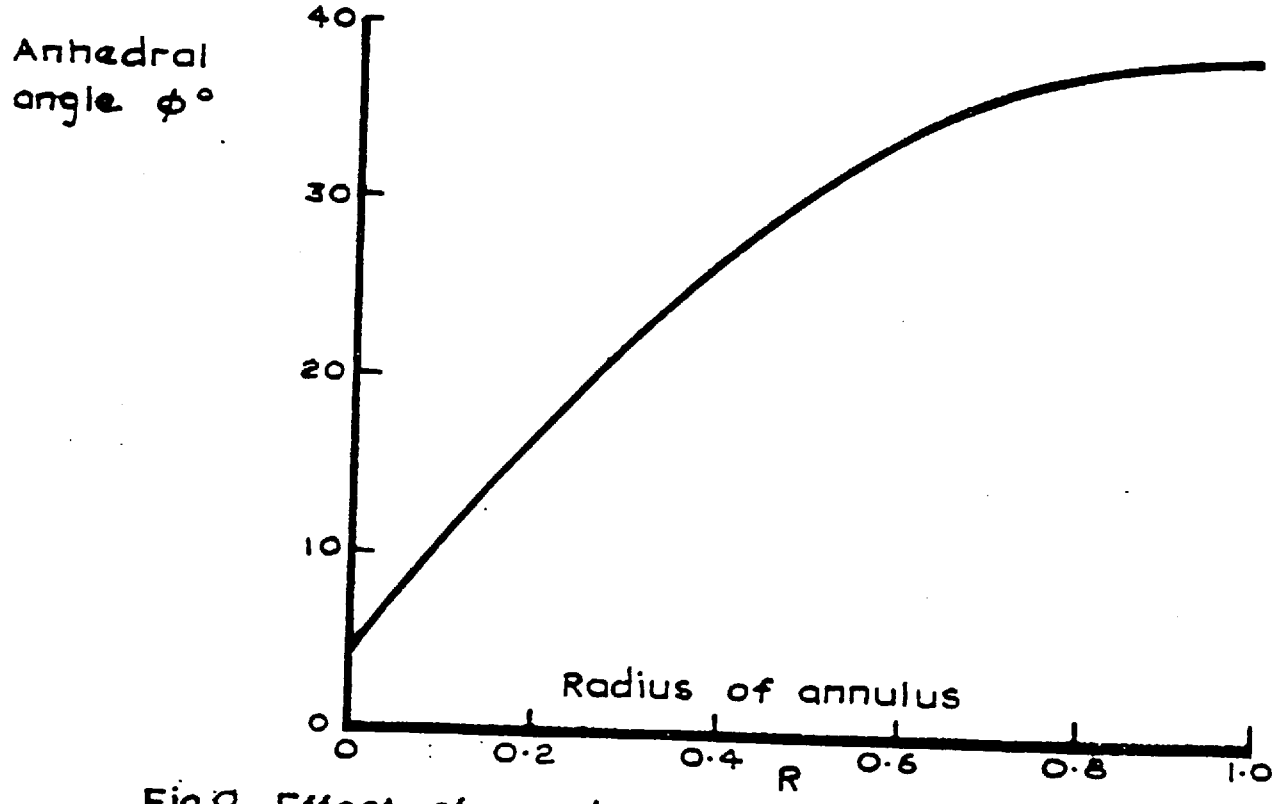

Fig.9 Effect of annular radius on ϕ and L/D

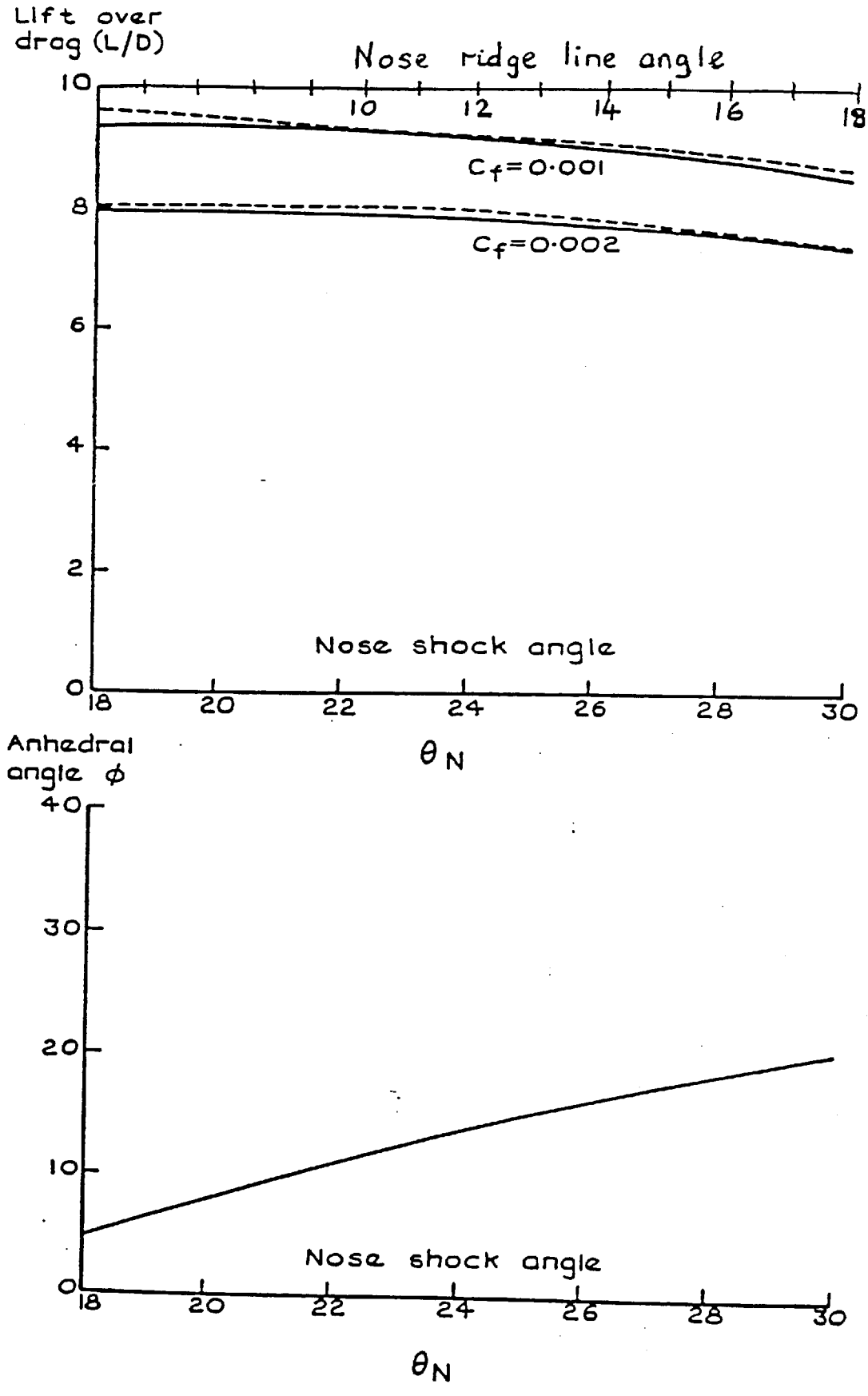

Fig. 10 Effect of nose shock angle on ϕ and L/D

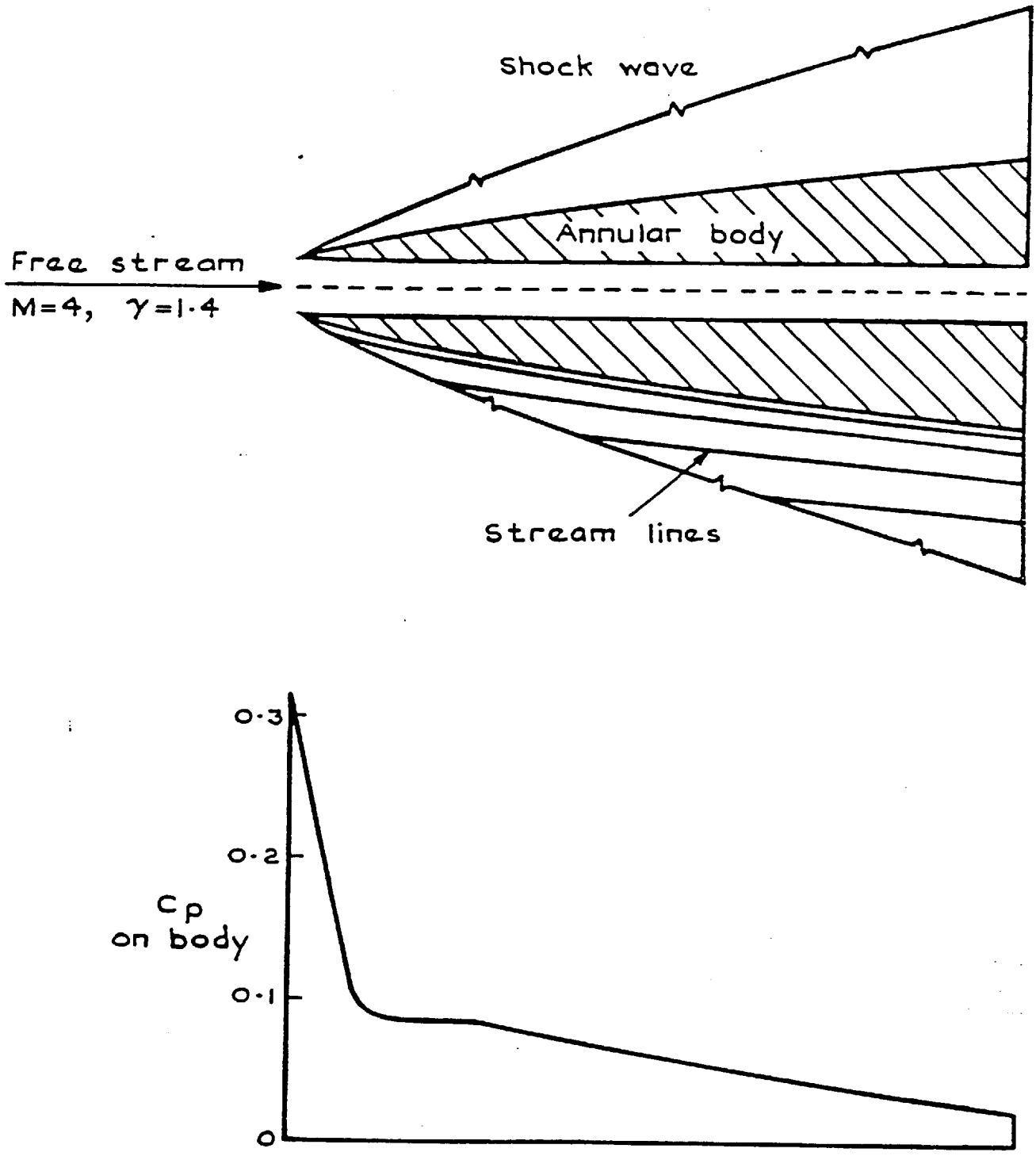

Fig. 11 Axisymmetric flow field with a 30° nose shock angle

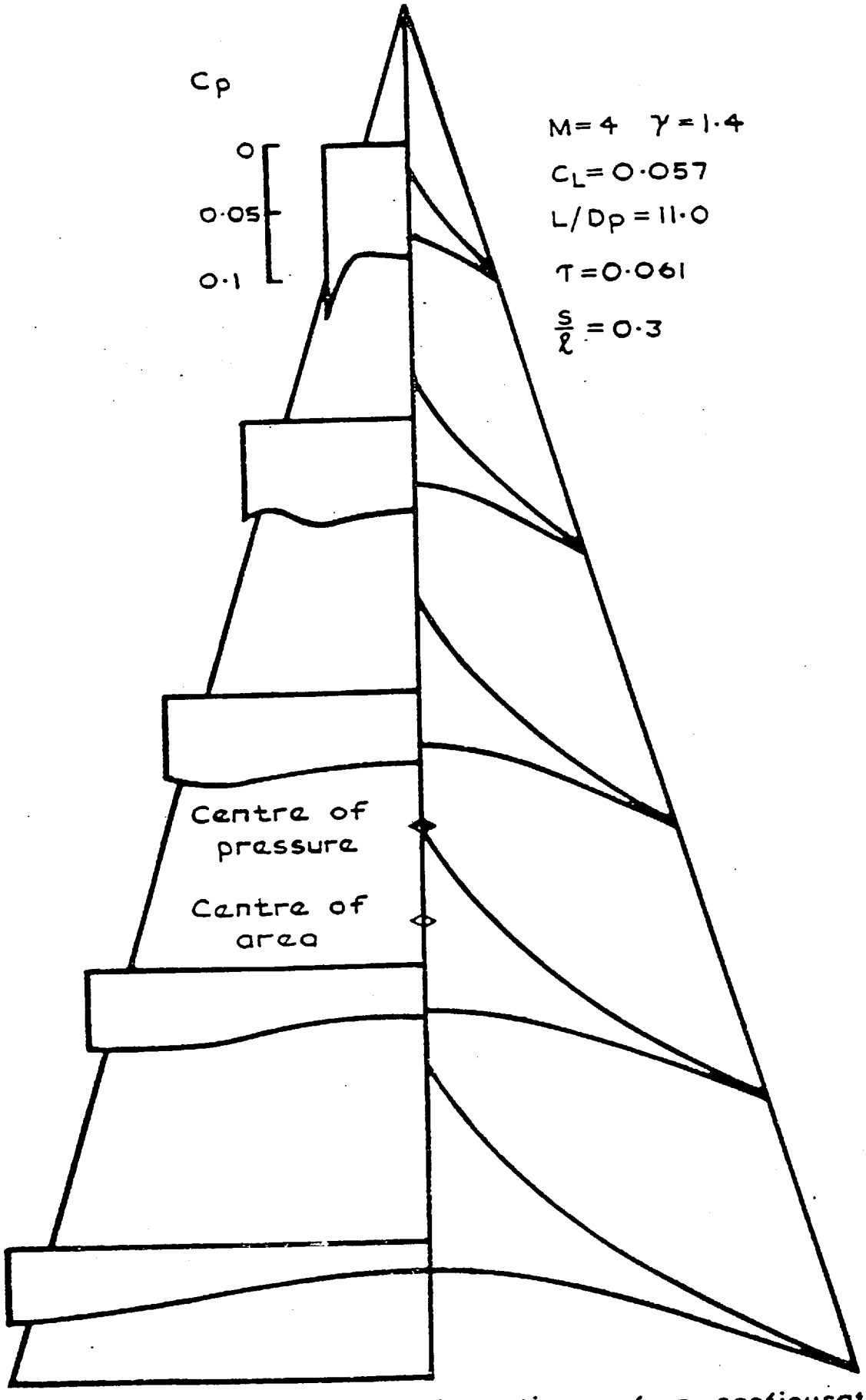

Fig.12 Pressure distribution and sections of a configuration derived from the flow field shown in Fig.11